JOURNAL OF SPACECRAFT AND ROCKETS
Vol. 39, No. 6, November–December 2002

Nonlinear Momentum Transfer Control of Spacecraft by Feedback Linearization

Hyochoong Bang,* Hyun-Sam Myung,† and Min-Jea Tahk‡
Korea Advanced Institute of Science and Technology, Daejon 305-701, Republic of Korea

The momentum transfer problem between a single momentum wheel and a rigid spacecraft is investigated. A feedback linearizing control is used for the momentum wheel. The proposed control law is a function of the spacecraft angular velocity vector components, as well as the inertia properties. The total initial angular momentum of the spacecraft is absorbed into the wheel, so that the spacecraft comes to rest at the steady state. The angular momentum component of the spacecraft and that of the wheel spin axis are selected as the primary control variables. A reference angular momentum history is predefined that leads to a smoothed control torque profile. The proposed control method produces a very small nutation angle at the completion of the momentum transfer maneuver. In addition, a two-stage control law switching strategy is proposed to complete the momentum transfer maneuver.

Nomenclature

H_T	=	magnitude of the total angular momentum, $\mathrm{N \cdot m \cdot s}$
$\hat{\boldsymbol{H}}_s$	=	angular momentum vector of the spacecraft, $\mathrm{N \cdot m \cdot s}$
$\hat{\boldsymbol{H}}_w$	=	angular momentum vector of the wheel, $\mathrm{N \cdot m \cdot s}$
h_w	=	angular momentum of the wheel relative to the spacecraft, $J_2\Omega$, $\mathrm{kg \cdot m^2/s}$
$I_i(I_i^* + J_i,$ $i = 1, 2, 3)$	=	total moments of inertia about each body axis, $\mathrm{kg \cdot m^2}$
(I_1^*, I_2^*, I_3^*)	=	principal moments of inertia of spacecraft, $\mathrm{kg \cdot m^2}$
$\tilde{I}_{12}$	=	$-(I_2 - I_1)/I_3$
$\tilde{I}_{23}$	=	$-(I_3 - I_2)/I_1$
$\tilde{I}_{31}$	=	$-(I_1 - I_3)/I_2$
(J_1, J_2, J_3)	=	principal moments of inertia of the wheel, $\mathrm{kg{\cdot}m^2}$
$L_f^k h(\boldsymbol{x})$	=	Lie derivative of $L_f^{(k-1)}h$ along f
$\hat{\boldsymbol{L}}$	=	external torque vector, $\mathrm{N \cdot m}$
N	=	magnitude of the applied torque, N
t	=	time, s
u	=	applied torque, $\mathrm{N \cdot m}$
$v(t)$	=	desired time history of the output function
$y(t)$	=	output to be controlled
$\delta()$	=	small perturbation of ( ) from equilibrium
Ω	=	wheel angular speed with respect to the spacecraft $\hat{\boldsymbol{b}}_2$ axis, rad/s
$(\omega_1, \omega_2, \omega_3)$	=	body frame angular velocity vector components, rad/s
ω_{30}	=	initial spin rate of spacecraft, rad/s
$\hat{\omega}(\omega_1\hat{\boldsymbol{b}}_1 + \omega_2\hat{\boldsymbol{b}}_2 + \omega_3\hat{\boldsymbol{b}}_3)$	=	angular velocity vector of spacecraft, rad/s

Received 31 October 2001; revision received 20 May 2002; accepted for publication 23 May 2002.

*Assistant Professor, Division of Aerospace Engineering, 373-1 Kusong-Dong, Yusong-Gu. Member AIAA.

†Graduate Student, Division of Aerospace Engineering, 373-1 Kusong-Dong, Yusong-Gu.

‡Professor, Division of Aerospace Engineering, 373-1 Kusong-Dong, Yusong-Gu. Member AIAA.

Introduction

A MOMENTUM transfer between spacecraft and internal wheels, in general, can be utilized to reorient spacecraft attitude.[1–3] The flat-spin recovery is an example for the momentum transfer.[3] The momentum wheels with torque command absorb the angular momentum of the spinning spacecraft. Attitude acquisition is achieved via momentum transfer using the principle of angular momentum conservation. The angular momentum vector is fixed in the inertial reference frame by the momentum conservation principle, so that the wheel spin axis under torque input tends to be aligned with the angular momentum vector absorbing the angular momentum of the spacecraft. The bias momentum spacecraft, in general, maintains a nominal angular speed at the mission orbit. In the early mission stage, the wheel speed needs to be set to a desired value that causes the spacecraft attitude to change in the course of wheel spin-up. Therefore, if the spacecraft attitude acquisition and angular momentum of the wheel is initialized simultaneously, it would be beneficial for various reasons. The 90-deg attitude acquisition, in conjunction with momentum wheel speed initialization to a nominal value, has been conducted in some bias momentum geostationary communication spacecraft missions.

A simple but very practical strategy for the momentum transfer is to apply constant torque[1,2] to the wheel, which is initially at rest. The wheel accelerates and the torque command is continued until the wheel angular momentum level reaches that of the whole system.[4,5] Once the wheel angular momentum level becomes close to the desired value, the torque command is removed, and the wheel comes into the so-called free wheeling state with a nearly constant speed. However, a constant torque input usually leads to residual oscillations about axes that are orthogonal to the wheel spin axis. The residual oscillation, in turn, produces an oscillating nutation error. Usually, passive damping is adopted to damp out such residual oscillations.[6,7] Thus, judicious choice of torque input to the wheel is an essential element for the satisfactory momentum transfer maneuver. The smaller the magnitude of the control torque is, in general, the smaller the anticipated nutation angle will be. However, the maneuver time tends to increases in such a case, and there is still no guarantee that desired transfer performance is feasible with very small torque.

Momentum transfer by optimal control theory has been studied in Ref. 4 by Vadali and Junkins. The momentum transfer condition was specified by the terminal conditions on angular velocity components. In other words, the residual oscillation at the end of a maneuver is minimized, while the integrated control energy is used as the performance index. A nonlinear two-point boundary value problem was solved to build an open-loop control. General dual-spin spacecraft stability and the associated core energy[6–9] principle have been employed to find out feedback forms of control commands for momentum transfer.[10,11] Weissberg and Ninomiya[10] used Hubert's core-energy concept to derive a feedback control control law, which is designed to decrease the core energy of a spacecraft with momentum wheels.[10] The core energy is defined to be the total system energy of a fictitious rigid body, neglecting the relative motion of the rotor. Kawaguchi et al.[12] applied an active control technique for the momentum transfer maneuver of multiwheel configuration. They designed a nonlinear feedback control law with a stability guarantee using Lyapunov's direct method. Hall[13] discussed a time-varying control torque input designed for two-rotor gyrostats. The so-called stationary-platform maneuver was developed, for which the platform angular velocity is minimized by an active control action.

A general approach for nonlinear systems is to first linearize the nonlinear systems about an equilibrium state. A linear controller is then designed for the linearized system. The accuracy of the lineriza-tion depends on how dominant the nonlinearity is about the equilibrium point. Depending on the state of the system, different equilibrium points may be needed to design different sets of linear control laws. One potential nonlinear control design technique is feedback linearization.[14–16] The feedback linearization is generally able to handle a nonlinearity more efficiently than conventional linearization techniques based on Jacobian linearization. An output function is defined first, and the controller is designed to make the output function follow a given reference trajectory. The control law consists of the reference and actual states of the system. The controller basically linearizes the system in the sense that stable tracking is achieved for the output function of the original nonlinear system.[15]

The principal objective of this study is to apply the feedback linearization technique to the momentum transfer of a spacecraft with single momentum wheel. The output function is defined as an angular momentum component of the spacecraft and the wheel. The output function is then used to derive a feedback control law in terms of angular velocity components and reference trajectory defined a priori. The reference trajectory generation is based on smoothed angular momentum transfer from the initial spin axis spacecraft into the final axis containing the wheel spin axis. The resultant controller produces smaller steady-state nutation errors compared to other previous approaches.[1,4] To resolve the case where the spacecraft body itself rotates even at the completion of the initial momentum transfer, the controller is switched into additional simple feedback controller. Therefore, the momentum wheel eventually absorbs the whole angular momentum of the system, so that spacecraft comes to rest almost completely. The proposed control law, therefore, provides performance enhancements in terms of final nutation error at the expense of complicated structure.

This paper is organized into several sections. First, a review is presented on essential principles of momentum transfer using a single momentum wheel. Then a brief review on feedback linearization theory is made, and the technique is applied to the momentum transfer maneuver.

Momentum Transfer for a Single Momentum Wheel

Formulations and Momentum Transfer Basics

To explain a typical momentum transfer between a single momentum wheel and a spacecraft, the spacecraft configuration shown in Fig. 1 is considered.

The spacecraft is initially spinning about the $\hat{\boldsymbol{b}}_3$ body axis. The momentum wheel is initially at rest so that the total angular momentum of the system corresponds to that of the spin about the $\hat{\boldsymbol{b}}_3$ axis. Now the momentum wheel starts to spin up, and the wheel angular momentum increases through control torque input. Because the total angular momentum of the system is constant in the inertial frame of reference, the angular momentum of the spacecraft is transferred into the wheel. As the wheel gains angular momentum, the wheel axis tends to be aligned with the angular momentum vector of the system that is fixed in the inertial frame.

The total angular momentum of the system is given by

$$\hat{\boldsymbol{H}} = \hat{\boldsymbol{H}}_s + \hat{\boldsymbol{H}}_w \tag{1}$$

Let us introduce the following notations for each term[5]:

$$\hat{\boldsymbol{H}}_s = I_1^*\omega_1\hat{\boldsymbol{b}}_1 + I_2^*\omega_2\hat{\boldsymbol{b}}_2 + I_3^*\omega_3\hat{\boldsymbol{b}}_3 \tag{2}$$

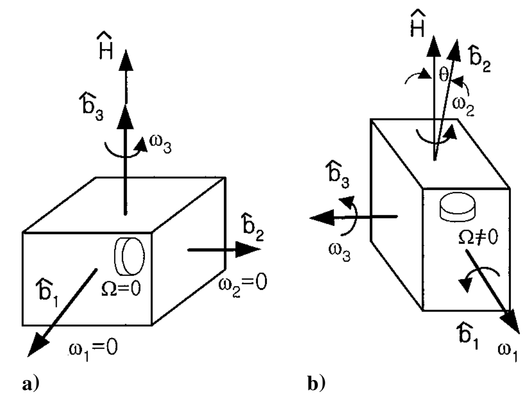

Fig. 1 Momentum transfer between spacecraft and a momentum wheel: a) initial spin and b) after momentum transfer.

$$\hat{\boldsymbol{H}}_w = J_1\omega_1\hat{\boldsymbol{b}}_1 + J_2(\omega_2 + \Omega)\hat{\boldsymbol{b}}_2 + J_3\omega_3\hat{\boldsymbol{b}}_3 \tag{3}$$

Thus, the total angular momentum of the system can be rewritten as

$$\hat{\boldsymbol{H}} = H_1\hat{\boldsymbol{b}}_1 + H_2\hat{\boldsymbol{b}}_2 + H_3\hat{\boldsymbol{b}}_3 \tag{4}$$

where the components are defined as

$$H_1 = I_1\omega_1, \qquad H_2 = I_2\omega_2 + h_w, \qquad H_3 = I_3\omega_3 \tag{5}$$

Based on the definition of the angular momentum of the system, the governing equations of motion are derived as

$$\left.\frac{\mathrm{d}\hat{\boldsymbol{H}}}{\mathrm{d}t}\right|_{\hat{b}} + \hat{\omega}\times\hat{\boldsymbol{H}} = \hat{\boldsymbol{L}} \tag{6}$$

For momentum transfer, the external torque input is set to zero, so that $\hat{\boldsymbol{L}} = \boldsymbol{0}$. Now, the preceding equations of motion can be rewritten in body frame as

$$I_1\dot{\omega}_1 + (I_3 - I_2)\omega_2\omega_3 - \omega_3 h_w = 0 \tag{7}$$

$$I_2\dot{\omega}_2 + (I_1 - I_3)\omega_3\omega_1 + \dot{h}_w = 0 \tag{8}$$

$$I_3\dot{\omega}_3 + (I_2 - I_1)\omega_1\omega_2 + \omega_1 h_w = 0 \tag{9}$$

In addition, the momentum wheel dynamics can be derived from applied torque and resultant angular momentum changes of the wheel about the $\hat{\boldsymbol{b}}_2$ axis[5]:

$$u = J_2(\dot{\omega}_2 + \dot{\Omega}) = J_2\dot{\omega}_2 + \dot{h}_w \tag{10}$$

Combining Eqs. (8) and (10) yields the wheel dynamics with respect to the wheel angular momentum[5]:

$$\dot{h}_w = \left(J_2/I_2^*\right)(I_1 - I_3)\omega_3\omega_1 + \left(I_2/I_2^*\right)u \tag{11}$$

Equation (8) can be rewritten in terms of the wheel torque as

$$I_2^*\dot{\omega}_2 + (I_1 - I_3)\omega_3\omega_1 + u = 0 \tag{12}$$

The preceding equations of motion alternatively can be put into a first-order state-space form

$$\dot{\boldsymbol{x}} = f(\boldsymbol{x}) + \boldsymbol{g}u \tag{13}$$

where the state vector is defined as

$$\boldsymbol{x} = [\omega_1, \omega_2, \omega_3, h_w]^T \tag{14}$$

Note that without an external torque input, the total angular momentum of the system is conserved, so that

$$H = \sqrt{H_1^2 + H_2^2 + H_3^2} \equiv H_T = \text{const} \tag{15}$$

As a convenient criterion for the momentum transfer, the nutation angle of the system can be defined as

$$\theta = \cos^{-1}(H_2/H) \tag{16}$$

Hence, the nutation angle decreases from 90 deg with H_2 equal to zero initially and a smaller value as the momentum transfer progresses. The smaller the final nutation angle is, the more successful maneuver performance is. Thus, the momentum transfer condition can be specified as

$$[\omega_1, \omega_2, \omega_3, h_w] = [0, 0, \omega_{30}, 0]$$

initially and

$$[\omega_1, \omega_2, \omega_3, h_w] = [0, 0, 0, J_2\Omega_f]$$

at final time. Here, Ω_f is the wheel angular rate that under ideal situation, corresponds to the angular momentum of the system scaled by inertial ratio.

A simple but practical momentum transfer strategy is to apply a constant torque input such as[1,2,4]

$$u(t) = N \tag{17}$$

When the constant torque is applied, the angular momentum of the wheel continues to grow until the input command is removed. The total angular momentum of the system is given by

$$H \equiv H_T = I_3\omega_{30} \tag{18}$$

The wheel torque command by Eq. (17) continues until

$$h_w = I_3\omega_{30} = H_T \tag{19}$$

is satisfied rigorously.

However, Eq. (19) only guarantees that the wheel has initial momentum magnitude and not necessarily the direction. The wheel angular momentum causes gyroscopic coupling about the $\hat{\boldsymbol{b}}_1$ and $\hat{\boldsymbol{b}}_3$ axes as implied by Eqs. (7) and (9), respectively. In addition, wheel control torque causes the angular velocity component ω_2 to change from Eq. (8). Residual oscillations, even after Eq. (19) is satisfied, are observed about every body axis. The degree of oscillations depends on the magnitude of the torque input.[1,4] In general, as the input magnitude N increases, the final nutation angle is likely to be trapped at a larger value.[5] Theoretically, a very small number for N could be selected, but maneuver time will increase in turn. Therefore, the best strategy is to find a control torque command that produces minimum residual angular motions at a reasonable amount of maneuver time.

A sample momentum transfer scenario has been simulated to illustrate the transfer strategy by constant torque input. Even though the constant torque input case has been extensively discussed in previous studies,[1,4,5] it would be a useful reference for the new control law to be introduced later. The moment of inertia data of the spacecraft model are given as $[I_1, I_2, I_3] = [86.24, 85.12, 113.59]\ \text{kg} \cdot \text{m}^2$ and $[I_1^*, I_2^*, I_3^*] = [86.215, 85.07, 113.565]\ \text{kg} \cdot \text{m}^2$, and an initial spin rate of 0.1771 rad/s about $\hat{\boldsymbol{b}}_3$ axis is chosen. For comparison with the previous study in Ref. 4, identical model data and simulation conditions are taken. The magnitude of the constant torque input is set to $N = 0.005(\text{N} \cdot \text{m})$, which is also equal to that of Ref. 4. Note that initial spin axis is the axis of maximum moment of inertia, whereas the wheel is aligned along the minimum moment of inertia axis. The moment of inertia for the initial spin axis is important for the successful transfer performance as discussed in the next section. Simulation results are presented in Fig. 2 with 4000-s simulation time.

The simulation results are exactly matched with those of Ref. 4. Torque input is applied until Eq. (19) is satisfied. The nutation angle decreases from 90 deg. The final nutation angle is shown to oscillate at about 7.7 deg. A significant amount of residual oscillations about other axes is also present.

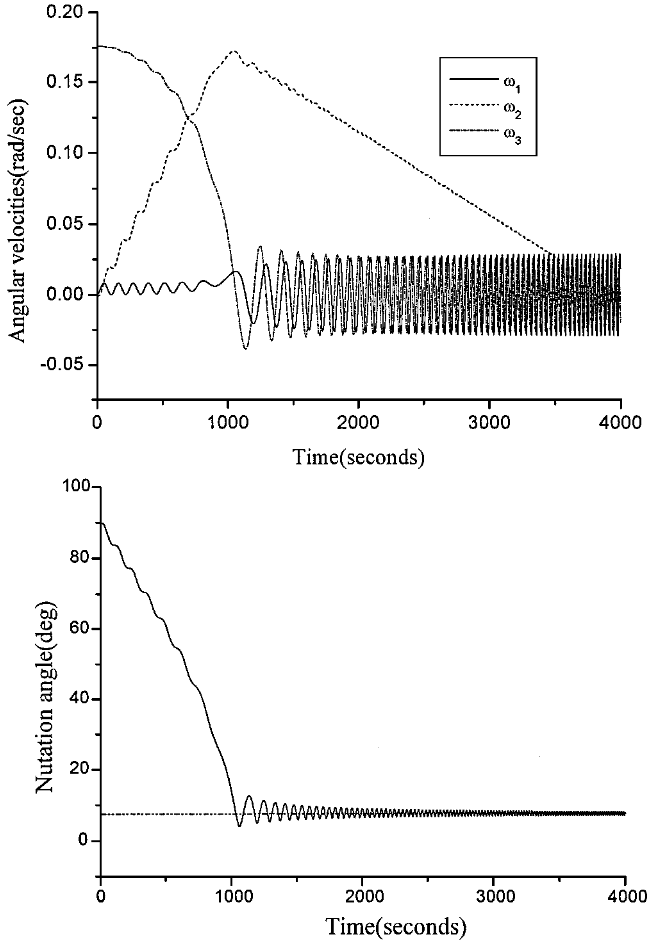

Fig. 2 Simulation results with constant torque input to the wheel.

Initial Stability

In the single wheel momentum transfer, the initial spin axis should be the maximum moment of inertia axis for a successful transfer. The moment of inertia taken in the preceding simulation satisfies $I_2 < I_1 < I_3$. If the initial spin axis happens to be an axis of minimum moment of inertia, then a so-called inverted turn[2,8] may result. In this case, the nutation angle increases over 90 deg combined with negative rotation ($\omega_2 < 0$) of the spacecraft body axis ($\hat{\boldsymbol{b}}_2$). An inverted turn may be prevented with a passive damper in Ref. 7. Even though the inverted turn is a fairly well-known phenomenon, a discussion on stability analysis is presented herein. It will provide an additional reference for the feedback linearization approach in the following section. In other words, whether the new feedback type control law can avoid the inverted turn will be examined.

The initial condition before momentum transfer action is prescribed as

$$\omega_1 = 0, \qquad \omega_2 = 0, \qquad \omega_3 = \omega_{30}, \qquad h_w = 0 \tag{20}$$

Then, by application of the torque command to the wheel, the following perturbed states are assumed to be created:

$$\omega_1 = \delta\omega_1, \qquad \omega_2 = \delta\omega_2, \qquad \omega_3 = \omega_{30} + \delta\omega_3$$
$$h_w = \delta h_w \tag{21}$$

where δ represents a small perturbation from the equilibrium state. The perturbed states are substituted into the original governing equations of motion, producing a set of linearized equations as

$$I_1\delta\dot{\omega}_1 + (I_3 - I_2)\omega_{30}\delta\omega_2 - \omega_{30}\delta h_w = 0 \tag{22}$$

$$I_2\delta\dot{\omega}_2 + (I_1 - I_3)\omega_{30}\delta\omega_1 + \delta\dot{h}_w = 0 \tag{23}$$

$$I_3\delta\dot{\omega}_3 = 0 \tag{24}$$

Note that $\delta\omega_3$ is nearly constant as demonstrated in the simulation results (Fig. 2). Furthermore, from Eq. (23),

$$\delta H_2 = I_2\delta\omega_2 + \delta h_w = -\int (I_1 - I_3)\omega_{30}\delta\omega_1\,\mathrm{d}t \tag{25}$$

Because $\omega_{30} > 0$, it follows that $\delta H_2 > 0$ when $I_3 > I_1$ and $\delta\omega_1 > 0$. From the definition of the nutation angle, the nutation angle should start to decrease if $\delta H_2 > 0$. This phenomenon is also evident from the simulation results. Now, to complement the analysis for the $\delta\omega_1 > 0$ condition, Eq. (22) can be rewritten as

$$I_1\delta\dot{\omega}_1 + [(I_3 - I_2)\delta\omega_2 - \delta h_w]\omega_{30} = 0 \tag{26}$$

Because $\delta h_w > 0$, it can be easily seen that $\delta h_w > (I_3 - I_2)\delta\omega_2$ needs to hold to assure $\delta\omega_1 > 0$. However, no conclusive remark on $\delta\omega_2$ can be made at this point. Rather than investigating $\delta\omega_2$ through extensive algebra work, we rely on the simulation results to show that $\delta\omega_1 > 0$ for the either maximum or minimum moment of inertia of the initial spin axis. Therefore, going back to Eq. (25), it can be stated that $\delta H_2 > 0$ with $\delta\omega_1 > 0$ at the initial perturbation, so that the nutation angle is expected to decrease from 90 deg.

On the other hand, if the original spin axis happens to be the axis of minimum moment of inertia such as $I_3 < I_1 < I_2$, an analogous analysis can be made. From Eq. (25), $I_3 - I_1 < 0$, and if we adopt the rigorous condition that $\delta\omega_1 > 0$ still holds as a verified simulation study regardless of the moment of inertia of the initial spin axis, it follows that $\delta H_2 < 0$ from Eq. (25). In such a case, the nutation angle exceeds 90 deg at the initial perturbation. Furthermore, $\delta\omega_2 < 0$ from Eq. (25), which is also verified by simulation. A nutation angle over 90 deg could be visualized by the wheel axis moving away from the angular momentum vector. In this case, the spacecraft body axis containing the wheel spins in the direction opposite ($\omega_2 < 0$) to the wheel spin direction.[2,5]

Unstable momentum transfer case is simulated with a different set of moment of inertia, given as $[I_1, I_2, I_3] = [86.24, 113.59, 85.12]\ \mathrm{kg\cdot m^2}$. The wheel spin axis corresponds to that of the maximum moment of inertias of the spacecraft. The torque input selected is identical to the previous simulation (Fig. 2). Numerical simulation results are provided in Fig. 3.

In contrast to the trend in Fig. 2, the nutation angle in this case starts to increase at the initial application of control command. The spacecraft body axis about the wheel axis tends to spin in the negative direction ($\omega_2 < 0$). The analysis made so far with constant torque input is connected to the feedback control in the following section.

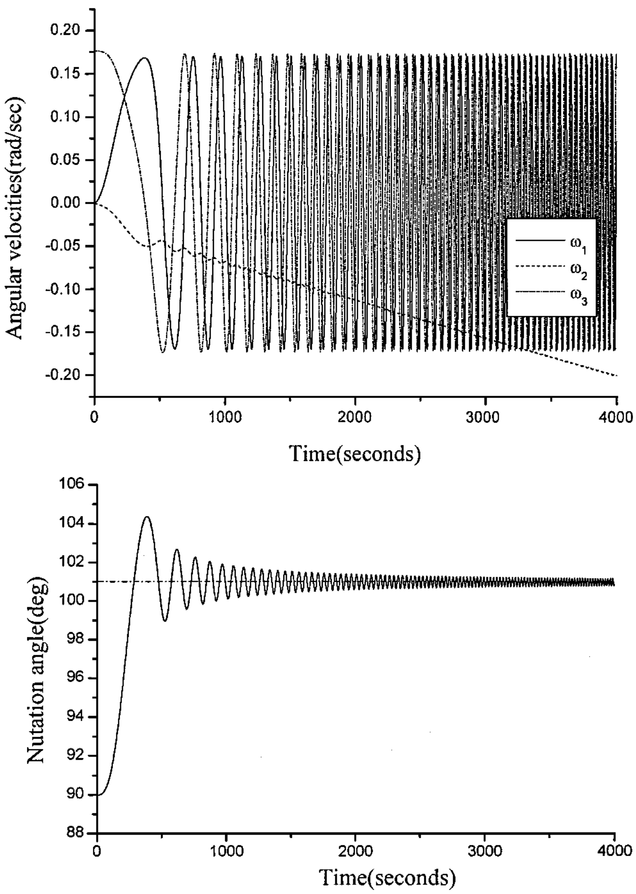

Fig. 3 Simulation results by unstable moment of inertia configuration.

Feedback Linearization

Before we design a momentum transfer control law by feedback linearization, we review the principal idea of feedback linearization. The majority of material on this section is from Ref. 15 by Lin. Other abundant material on feedback linearization is also available, but most of it is not listed in this study for the sake of brevity. As noted before, the feedback linearization technique is based on a linearized relationship between input and output. For an n-dimensional single-input/single-output nonlinear system of the form[15]

$$\dot{\boldsymbol{x}} = \boldsymbol{f}(\boldsymbol{x}) + \boldsymbol{g}(\boldsymbol{x})u \tag{27}$$

the output function is defined as

$$y(t) = h[\boldsymbol{x}(t)] \tag{28}$$

where $\boldsymbol{f}(\boldsymbol{x})$ and $\boldsymbol{g}(\boldsymbol{x})$ are functions of vector fields in R^n.

The feedback linearization is to find an integer ρ and a feedback control of the form

$$u = \alpha(\boldsymbol{x}) + \beta(\boldsymbol{x})v \tag{29}$$

where α and β are smooth functions defined in a neighborhood of some point $\boldsymbol{x}_0 \in R^n$ and $\beta(\boldsymbol{x}_0) \neq 0$ such that the closed-loop system by the control input

$$\dot{\boldsymbol{x}} = f(\boldsymbol{x}) + g(\boldsymbol{x})\alpha(\boldsymbol{x}) + g(\boldsymbol{x})\beta(\boldsymbol{x})v \tag{30}$$

$$y = h(\boldsymbol{x}) \tag{31}$$

has the property that the ρth-order derivative of the output is given by

$$y^{(\rho)}(t) = v(t) \tag{32}$$

The generalized form of the system given in Eqs. (27) and (28) is input–output linearizable around $\boldsymbol{x}_0$ with relative degree ρ by the following expression for the control law[15]:

$$u(t) = \frac{-L_f^{\rho}h(\boldsymbol{x}) + v}{L_g L_f^{(\rho-1)}[h(\boldsymbol{x})]} \tag{33}$$

for which the output function satisfies

$$y^{(\rho)}(t) = v(t) \tag{34}$$

so that the system is assumed to have a relative degree ρ at $\boldsymbol{x}_0$. $L_f^k h(\boldsymbol{x})$ is the Lie derivative, satisfying $L_f^0 = h$, $L_f h = (\partial h/\partial x) f(x)$, and $L_f^k h(x) = (\partial L_f^{(k-1)} h/\partial x) f(x)$ (Ref. 15).

Now, for the feedback control law, exact tracking of the output signal is realized if the error signal is defined as

$$e(t) = y(t) - y_d(t) \tag{35}$$

and it satisfies

$$y^{(\rho)}(t) = y_d^{(\rho)}(t) = v(t) \tag{36}$$

together with $e^{(j)}(0) = 0$, $j = 1, 2, \ldots, \rho - 1$. The control input then should be of the form

$$u(t) = \frac{-L_f^{\rho}h[\boldsymbol{x}(t)] + y_d^{(\rho)}(t)}{L_g L_f^{(\rho-1)}h[\boldsymbol{x}(t)]} \tag{37}$$

The control law design can be further extended into an asymptotic tracking control. In other words, the control law

$$v(t) = r^{(\rho)}(t) - \left[\alpha_{(\rho-1)}e^{(\rho-1)} + \cdots + \alpha_1 e^{(1)}(t) + \alpha_0 e(t)\right] \tag{38}$$

results in a closed-loop system dynamics:

$$e^{(\rho)} + \alpha_{(\rho-1)}e^{(\rho-1)}(t) + \cdots + \alpha_1 e^{(1)}(t) + \alpha_0 e(t) = 0 \tag{39}$$

for the output function. The parameters $\alpha_{(i)}$, $i = 0, 1, \ldots, \rho - 1$, should be selected in such a way to guarantee stability of the closed-loop system. In this case, the control law is expressed in the form

$$u(t) = \frac{-L_f^\rho h[\mathbf{x}(t)] + r^{(\rho)}(t) - \sum_{k=0}^{\rho-1} \alpha_k e^{(k)}(t)}{L_g L_f^{(\rho-1)} h[\mathbf{x}(t)]} \tag{40}$$

Obviously, the asymptotic closed-loop tracking control law is more practical than the exact open-loop control law considering the initial error between the reference and actual system in general cases.

Momentum Transfer by Feedback Linearization

Control Law Design by Feedback Linearization

As a choice for the output function in feedback linearziation for the momentum transfer, the wheel angular momentum can be selected:

$$y = h_w \tag{41}$$

Furthermore,

$$\dot{y} = \dot{h}_w \simeq u \tag{42}$$

from Eq. (10) because $\dot{\omega}_2$ is generally much smaller compared to wheel angular acceleration. Thus, the controller could be determined trivially as the input torque to the wheel. However, this case again reduces to the original open-loop problem for which the control input should be determined judiciously for optimum performance. Even if we could arbitrarily specify the control input, an open question would remain as to how to select the control torque profile. The wheel command torque alone does not guarantee desired performance as illustrated in the constant torque input case.

Next, we propose another candidate output function as

$$y = H_2 = I_2\omega_2 + h_w \tag{43}$$

It is based on the idea that the nutation angle depends on the angular momentum about the $\hat{\boldsymbol{b}}_2$ axis because the total angular momentum is conserved. From the definition of the nutation angle in Eq. (16), it can be claimed that as the output function ($y = H_2$) reaches the total angular momentum, the nutation angle also approaches zero.

With the output function defined, we take successive differentiation so that the relative degree is determined first. Now, from Eq. (8), it can be easily shown that

$$\dot{y} = -(I_1 - I_3)\omega_1\omega_3 \tag{44}$$

The control input dose not explicitly appear in $\dot{y}$; thus, one more differentiation is taken to yield

$$\ddot{y} = -(I_1 - I_3)(\dot{\omega}_1\omega_3 + \omega_1\dot{\omega}_3) \tag{45}$$

Now, substituting Eqs. (7) and (9) into Eq. (45) and rearranging terms leads us to

$$\ddot{y}/(-I_1 + I_3) = (\tilde{I}_{23}\omega_2 + h_w/I_1)\omega_3^2 + (\tilde{I}_{12}\omega_2 - h_w/I_3)\omega_1^2 \tag{46}$$

The second derivative of the output function still does not show direct dependency on the control input. Thus, an additional step is taken to produce

$$\begin{aligned} y^{(3)}\big/(-I_1 + I_3) = {} & \tilde{I}_{31}\big[(\tilde{I}_{23} - h_w/I_1)\omega_3^2 + (\tilde{I}_{12} + h_w/I_3)\omega_1^2\big]\omega_1\omega_3 \\ & + 4\omega_1\omega_3[\tilde{I}_{23}\omega_2 + h_w/I_1][\tilde{I}_{23}\omega_2 - h_w/I_3] \\ & + \big[\big(1/I_1 - \tilde{I}_{23}\big/I_2^*\big)\omega_3^2 + \big(-1/I_3 - \tilde{I}_{12}\big/I_2^*\big)\omega_1^2\big]u \end{aligned} \tag{47}$$

The third-order derivative of the output ($y^{(3)}$) contains the control input explicitly. Therefore, the relative degree (ρ) is equal to three. The preceding equation can be rewritten in new symbols as

$$y^{(3)} \equiv P(\omega_1, \omega_2, \omega_3) + Q(\omega_1, \omega_3)u \tag{48}$$

Now, to design a control law based on the explicit relationship between the third-order derivative of the output and the control input, a reference trajectory of the output function needs to be generated.

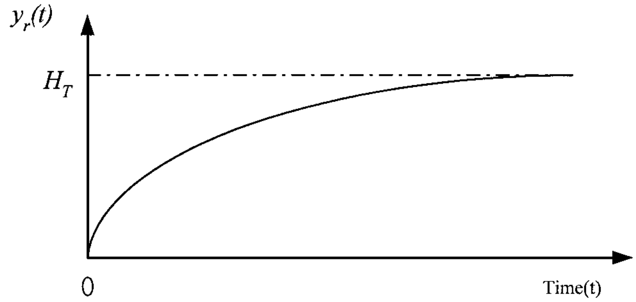

Fig. 4 Reference angular momentum trajectory.

The reference output is taken as the reference angular momentum to be tracked by the output function (H_2). Mathematically, it is given in the form

$$y_r = H_T[1 - \exp(-t/\tau)] \tag{49}$$

where H_T again represents the total angular momentum of the system, and τ is a time constant determining the shape of the reference trajectory. The reference angular momentum trajectory is graphically represented in Fig. 4.

Obviously, there could be other choices of the reference angular momentum profile. However, the reference angular momentum selected here implies that the whole angular momentum of the system is absorbed into the $\hat{\boldsymbol{b}}_2$ axis at the steady state. Consequently, it corresponds to the nutation angle converging to zero at the steady state if the actual angular momentum (H_2) tracks the reference trajectory within reasonable accuracy. The time derivatives of the reference signal are given as

$$\dot{y}_r = H_T/\tau \exp(-t/\tau) \tag{50}$$

$$\ddot{y}_r = -H_T\big/\tau^2 \exp(-t/\tau) \tag{51}$$

$$y_r^{(3)} = H_T\big/\tau^3 \exp(-t/\tau) \tag{52}$$

Now the third-order derivative of the output in Eq. (47) is utilized to define a single-input and single-output system:

$$\begin{aligned} y^{(3)} &= v(t) = y_r^{(3)} \\ &= P(\omega_1, \omega_2, \omega_3) + Q(\omega_1, \omega_3)u \end{aligned} \tag{53}$$

The equation could be used to find the control command explicitly in terms of the reference trajectory, spacecraft mass properties, and angular velocity components. From Eq. (53), note that the control input depends on spacecraft angular velocity components ($\omega_1, \omega_2, \omega_3$), which nowdays are measurable by onboard inertial measurement units. From a physical point of view, the controller attempts to control angular momentum components orthogonal to the $\hat{\boldsymbol{b}}_2$ body axis.

The feedback linearization is known to be useful in handling a given output function tracking performance by feedback control. Because the principal objective of the momentum transfer is to control the angular momentum component along the wheel and/or spacecraft body ($\hat{\boldsymbol{b}}_2$) axis, the total angular momentum ($y = I_2\omega_2 + h_w$) is selected at the output function. Then, the output function is prescribed to follow a smooth reference trajectory, which is expected to produce a small nutation angle at the maneuver end. The control input is directly related to the desired output trajectory through a feedback linearization technique. In the approaches shown earlier, there is no direct connection between the control input and the angular momentum ($y = I_2\omega_2 + h_w$). Therefore, the feedback linearization approach in this study results in more active control of the angular momentum or nutation angle profile.

Asymptotic Tracking

The time derivatives of the output and reference trajectories derived in the earlier part of this paper can be combined together to build an asymptotic tracking control law. From the generalized form of the tracking control law in Eq. (40), a tracking controller is proposed as

$$u(t) = [v - P - \alpha_2(\ddot{y} - \ddot{y}_r) - \alpha_1(\dot{y} - \dot{y}_r) - \alpha_0(y - y_r)]/Q \tag{54}$$

Application of the preceding tracking controller produces a stable output response governed by

$$e(t)^{(3)} + \alpha_2\ddot{e}(t) + \alpha_1\dot{e}(t) + \alpha_0 e(t) = 0 \tag{55}$$

where $e(t) = y(t) - y_r(t)$ represents error between the actual and reference outputs. The design parameters α_i $(i = 0, 1, 2)$ should be selected to produce a stable closed-loop system.

Simulation

A momentum transfer scenario is simulated with the proposed control law. The tracking control torque command is, therefore, applied to a model spacecraft that is identical to that in the earlier case of constant torque input. To avoid unusually excessive control command, a limiter is implemented as

$$dsu(t) = \begin{cases} N & \text{if} \quad u(t) > N \\ u & \text{if} \quad -N < u(t) < N \\ -N & \text{if} \quad u(t) < -N \end{cases} \tag{56}$$

where N is set equal to the constant torque input magnitude of $0.005\ \text{N} \cdot \text{m}$. Design parameters α_i in Eq. (55) and a time constant of reference trajectory are selected by a few trials. Simulation results produced by the new tracking control law is presented in Fig. 5.

Compared to the simulation results in Fig. 2, the new control law can be shown to absorb the initial angular momentum of the spacecraft more effectively. Angular velocity components about the $\hat{\boldsymbol{b}}_1$ and $\hat{\boldsymbol{b}}_3$ axes converge to very small numbers without much oscillation. Small residual oscillation is a significant improvement in terms of final nutation angle over the conventional constant torque input cases in Refs. 1 and 4. The final nutation angle in Fig. 2 oscillates around 7.7 deg with constant input. The optimal control approach in Ref. 4 produced a final nutation angle of 4.2 deg. Now the nutation angle error by the new control law is about 0.1 deg, only over the same maneuver time. Obviously, such significant improvement in nutation error by the new control law is made possible by a complicated controller structure using feedback instead of open-loop control. Despite a much smaller nutation angle, the proposed controller structure is more complicated compared to preceding open-loop approaches. The constant and optimal control torque input could have a certain limitation in minimizing the nutation angle compared to the feedback control in this study. However, the principal advantage of the preceding methods lies in the simpler implementation of the controller. Therefore, the simplicity of the controller and small nutation angle by feedback control could be a tradeoff subject in actual applications.

The reason for such a small nutation angle may be due to the smoothed reference trajectory of the output function. The output function is prescribed to follow the given trajectory, which seemingly leads to a smooth nutation angle trend. The smoothed reference trajectory produced a smoothed time-varying control command with corresponding smooth momentum transfer. As the final nutation angle becomes smaller, the residual oscillations ω_1 and ω_3 should become smaller in proportion. The output feedback linearization approach connects the output function directly to the control input in a stable manner, so that more active control of the nutation angle by using the predefined reference trajectory is achieved. The mathematical analysis of ω_1 and ω_3 is not simple because the closed-loop system with the applied control input is highly nonlinear. Instead, the smaller nutation angle provides a conjecture on the magnitude of ω_1 and ω_3 because it is validated by nonlinear simulation results.

The control input starts from a nonzero value and converges to zero. Around the final simulation time, for some combinations of design parameters, a numerical difficulty has taken place. The difficulty turns out to be the case where the numerator and denominator in Eq. (54) approaches the zero line around the final simulation time. From physical view point, the control input should be continuous,

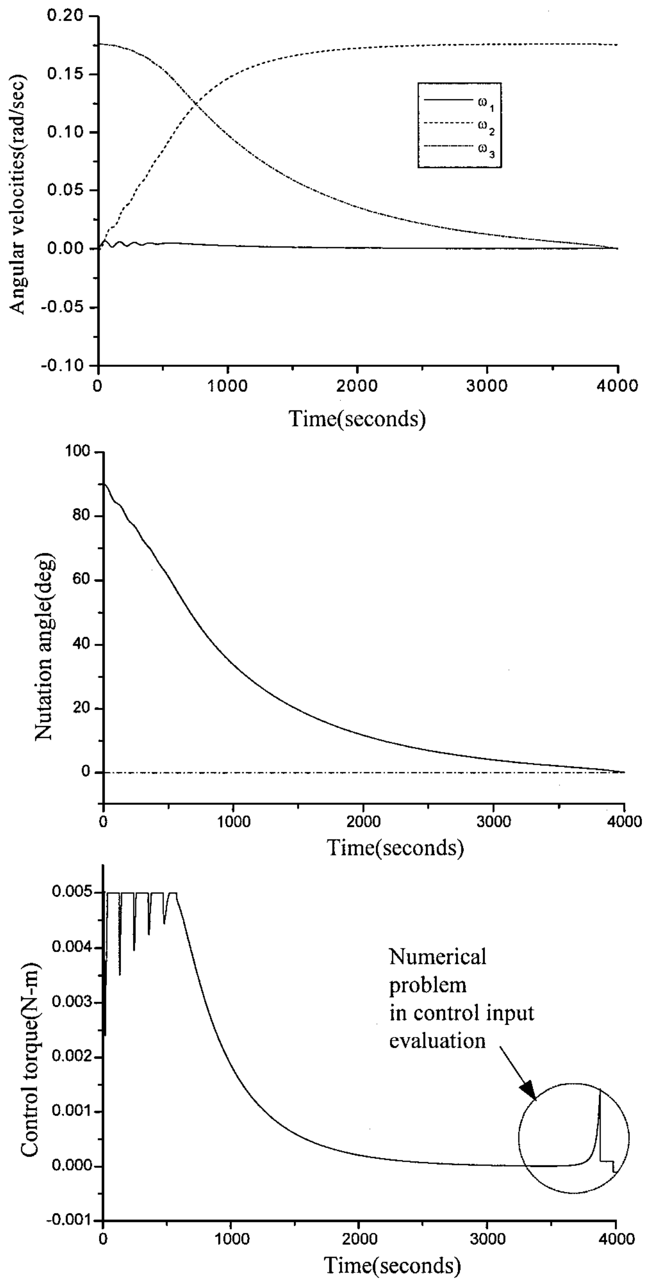

Fig. 5 Simulation results with feedback linearization control torque input.

with a finite value. The sharp rise of control command at the end of simulation time, therefore, has been handled by an appropriate switching technique by monitoring whatever numerical instability exists at steady state. Nevertheless, such a problem could be avoided by examining those terms before issuing the control command to be delivered. When it is intended to tolerate a bigger final nutation error by stopping the control action earlier, control command does not experience the computational problem.

Another point to be addressed is that, even if the final nutation angle itself is relatively small, the spacecraft body rotates as indicated by the steady-state angular velocity ω_2 about the $\hat{\boldsymbol{b}}_2$ axis. This is because of the structure of the output function defined in Eq. (43). The control law alone is not able to distribute the angular momentum into the wheel only. Consequently, the spacecraft spinning motion is locked with the wheel rotating together in the $\hat{\boldsymbol{b}}_2$ axis. Therefore, to transfer the angular momentum soley into the momentum wheel, an additional control strategy should be considered that will be discussed in the next section.

In the preceding section, it was discussed that the moment of inertia of the initial spin axis plays a central role for the momentum transfer results. Initial spin about the minimum moment of inertia

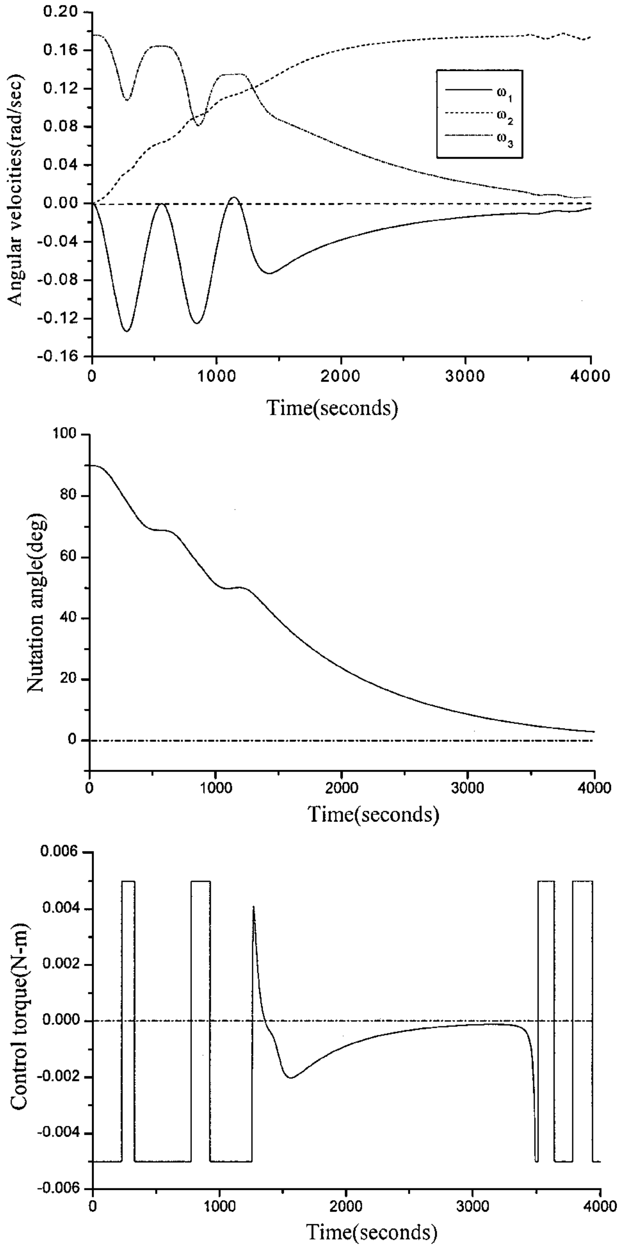

Fig. 6 Output responses by feedback linearized control input for unstable momentum of inertia configuration.

axis produces an unstable response with same torque input, producing a nutation angle that is finally trapped into an incorrect attitude. Now, the new control strategy by feedback linearization is illustrated over such a case by a simulation study. The set of moment of inertias is $[I_1, I_2, I_3] = [86.24, 113.59, 85.12]\ \mathrm{kg\cdot m^2}$, an unstable configuration in the preceding constant torque input study. Identical control command governed by Eq. (54) is applied with the new moment of inertia set. The maximum control torque is also limited to the same value as Eq. (56). The simulation outputs are shown in Fig. 6.

The nutation angle, in contrast to the case with constant torque input, tends to decrease. The controller tries to control the output function, and the moment of inertia is automatically taken into account in the control law. As can be shown, the initial sign of control command is negative, being opposite to the stable case. The control command history shows trends wilder than the stable case. Numerical problems in evaluation of the control command are attributed to the source of such a trend.

Switching Control Law

In the earlier simulation work, it was shown that a small nutation angle was achieved. This implies that the spacecraft angular momentum is transferred into the $\hat{b}_2$ axis successively. However, the final spacecraft angular velocity ω_2 about the $\hat{b}_2$ axis does not converge to zero. The output function is not intelligent enough to distribute angular momentum into the wheel only. To complete the momentum transfer maneuver, it is necessary to transfer every angular momentum of the spacecraft into the wheel. In order words, the spacecraft is required to be stopped almost completely. Thus, the final condition after momentum transfer should be as close as

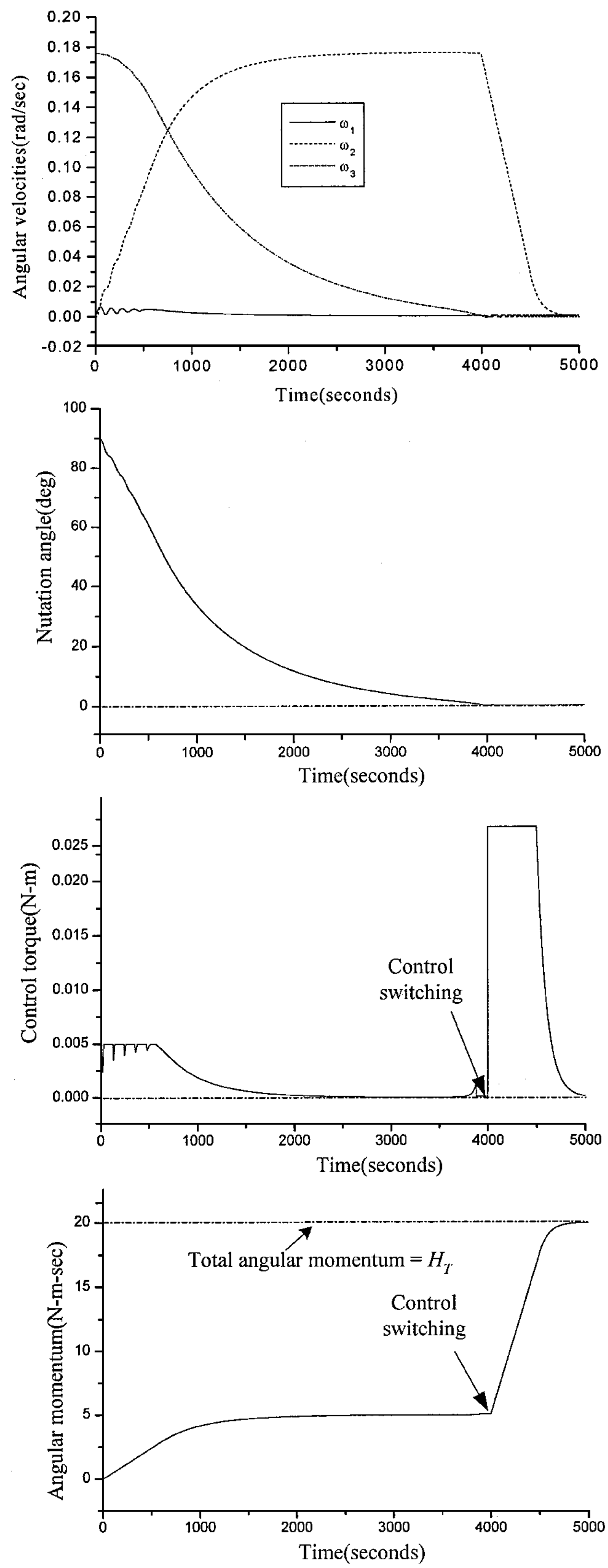

Fig. 7 Simulation responses with switching control law.

possible to

$$(\omega_1, \omega_2, \omega_3, \Omega) = (0, 0, 0, \Omega_f)$$

Now, motivated by the final nutation angle given by the proposed control law being small enough so that gyroscopic effects about the $\hat{\boldsymbol{b}}_1$ and $\hat{\boldsymbol{b}}_3$ axes are negligible, an additional wheel control law is proposed:

$$u = \gamma\omega_2, \qquad \gamma > 0 \tag{57}$$

The idea for the proposed control law is that the spacecraft, with a very small nutation error, is at nearly a pure-spin condition in the $\hat{\boldsymbol{b}}_2$ axis by the feedback linearized control. Therefore, the control action [Eq. (57)] is simply required to slow the spacecraft spin rate in that axis. The preceding control law, therefore, becomes operational after the final nutation angle reaches a threshold value by application of the feedback control law. The control law, when substituted into the original equation of motion [Eq. (8)] on the condition of small residual oscillations about orthogonal body axes $\hat{\boldsymbol{b}}_1$ and $\hat{\boldsymbol{b}}_3$, yields

$$I_2^*\dot{\omega}_2 + \gamma\omega_2 = 0 \tag{58}$$

Now the spacecraft angular velocity ω_2 becomes a stable first-order system. Because the total angular momentum of the system is constant, the wheel angular momentum should change at the same rate as that of the spacecraft. Considering that the small residual oscillations about orthogonal axes, it can be stated that the momentum wheel eventually will absorb the total angular momentum of the system.

Momentum transfer with the control switching strategy has been simulated with the results presented in Fig. 7. The simulation time is extended by 1000 s to allow enough time for the switched control command to be in effect.

Simulation results show that the spacecraft body finally reaches almost negligible angular velocity levels in all body axes. The wheel absorbs all of the angular momentum of the system. In particular, the spacecraft body angular momentum about the $\hat{\boldsymbol{b}}_2$ axis is quickly transferred into the wheel after the new control law is activated at 4000 s. The residual oscillation due to the switched control law is still far less than the constant torque case; specifically, it is less than at least 10% in angular velocity about the $\hat{\boldsymbol{b}}_1$ axis compared to those in Refs. 1 and 4. The steady-state nutation angle oscillates at about as small as 0.2 deg. The large torque (i.e., large γ at the instant of switching into another control law) is introduced to show that large torque input could be applied without inducing excessive gyroscopic coupling. Large torque has been generally prohibited in traditional momentum transfer strategies to reduce large nutation error, but it is accommodated in this case with a small nutation error.

Conclusions

Feedback linearization technique has been applied to a single wheel momentum transfer problem. The new control command consists of nonlinear combinations of angular velocity components and inertial properties of a spacecraft. The proposed control law was able to achieve a highly satisfactory momentum transfer, producing a very small nutation angle at the steady state. The control law automatically handles the case where initial spin axis is the minimum moment of inertia axis. However, it turns out that the body axis along the wheel rotates locked with the wheel, and angular momentum is not completely absorbed into the wheel. This problem was solved by introducing a two-stage switching control strategy. The combined feedback linearization and additional control action achieve a satisfactory momentum transfer mission. Robustness and practical implementation issues for the proposed control law need to be followed in future study.

References

[1]Barba, P., and Aubrun, J., "Satellite Attitude Acquisition by Momentum Transfer," American Astronautical Society, Paper AAS-75-053, July 1975.

[2]Kaplan, M., *Modern Spacecraft Dynamics and Control*, 1st ed., Wiley, New York, 1976, pp. 367–379.

[3]Gebman, G., and Mingori, T., "Perturbation Solution for the Flat Spin Recovery of a Dual-Spin Spacecraft," *AIAA Journal*, Vol. 14, No. 7, 1976, pp. 859–867.

[4]Vadali, S. R., and Junkins, J. L., "Spacecraft Large Angle Rotational Maneuvers with Optimal Momentum Transfer," AIAA Paper 82-1469, Aug. 1982.

[5]Junkins, J. L., and Turner, J. D., *Optimal Spacecraft Rotational Maneuvers*, 1st ed., Elsevier, Amsterdam, 1986, pp. 267–287.

[6]Kane, T. R., and Levinson, D. A., "Energy-Sink Analysis of Systems Containing Driven Rotors," *Journal of Guidance, Control, and Dynamics*, Vol. 3, No. 3, 1980, pp. 234–238.

[7]Hubert, C., "Spacecraft Attitude Acquisition from an Arbitrary Spinning or Tumbling State," *Journal of Guidance, Control, and Dynamics*, Vol. 4, No. 2, 1981, pp. 164–170.

[8]Cochran, J. E., and Shu, P. H., "Effects of Energy Addition and Dissipation on Dual-Spin Spacecraft Attitude Motion," *Journal of Guidance, Control, and Dynamics*, Vol. 6, No. 5, 1983, pp. 368–373.

[9]Ross, I. M., "Nutational Stability and Core Energy of a Quasirigid Gyrostat," *Journal of Guidance, Control, and Dynamics*, Vol. 16, No. 4, 1993, pp. 641–647.

[10]Weissberg, J., and Ninomiya, K., "Improved Method for the Initial Attitude Acquisition Maneuver," *Journal of Guidance, Control, and Dynamics*, Vol. 10, No. 3, 1987, pp. 316–319.

[11]Bang, H., Kim, S., and Hwangbo, H., "Feedback Control Law Design for the Dual-Spin Turn of Spacecraft," *Journal of Guidance, Control, and Dynamics*, Vol. 20, No. 3, 1997, pp. 450–456.

[12]Kawaguchi, J., Maeda, K., Matsuo, H., and Ninomiya, K., "Closed-Loop Momentum Transfer Maneuvers Using Multiwheels," *Journal of Guidance, Control, and Dynamics*, Vol. 18, No. 4, 1995, pp. 867–874.

[13]Hall, C. D., "Momentum Transfer in Tow-Rotor Gyrostats," *Journal of Guidance, Control, and Dynamics*, Vol. 19, No. 5, 1996, pp. 1157–1161.

[14]Snell, S. A., Enns, S. D., and Garrard, W. L., Jr., "Nonlinear Inversion Flight Control for a Supermaneuverable Aircraft," *Journal of Guidance, Control, and Dynamics*, Vol. 15, No. 4, 1992, pp. 976–984.

[15]Lin, C. F., *Advanced Control Systems Design*, Prentice–Hall, Upper Saddle River, NJ, 1994, pp. 263–284.

[16]Schumacher, C., "Stability Analysis of a Missile Control System with a Dynamics Inversion Controller," *Journal of Guidance, Control, and Dynamics*, Vol. 21, No. 3, 1998, pp. 508–515.

D. B. Spencer
Associate Editor